JOURNAL OF CATALYSIS 11, 283–294 (1968)

Adsorption of Carbon-14 Labeled Formic Acid on Silver Films of Small Area

A. LAWSON

From the Commonwealth Scientific and Industrial Research Organization, Division of Tribophysics, University of Melbourne, Australia

Received February 7, 1968

A radiotracer technique is described for measuring the adsorption of $H^{14}COOH$ on surfaces of Pyrex, mica, and silver at room temperature, and pressures of 10^{-3}–10^{-1} torr. The technique is sufficiently sensitive that low coverages (10^{13} mols./cm^2) can be measured on surfaces of a few square centimeters. At low pressures the adsorption is strong and largely irreversible at room temperature; at pressures above 1×10^{-2} torr there is additional weak and completely reversible adsorption beyond that of a Langmuir monolayer of the strongly bound species. Adsorption measurements on polycrystalline and (111) epitaxed films of silver on mica are described, and from estimates of the proportions of (111) area in the samples, the coverage is calculated for the atomically smooth (111) plane alone, and for the atomically rough surface. The coverage on the rough surface is that expected for close-packed adsorption of freely rotating ions; the coverage on the (111) plane is very low, and the reasons for this are discussed.

Introduction

Adsorption studies of formic acid on metals have so far been restricted to measurements on either powders or polycrystalline materials. On nickel and copper, measurements under reaction conditions showed that the coverages were high, and on nickel two formic acid molecules were absorbed to every nickel atom on the surface (*1, 2*). On the more noble metals such as silver, Tamaru (*2*) found the coverages to be considerably lower and only one formic acid molecule was adsorbed to every 10 silver atoms on the surface. Similarly, Sachtler and Fahrenfort (*3*) found coverages to be low on gold at room temperature, but their measurements were close to the limits of resolution of conventional adsorption apparatus. It seemed desirable to have more information about the coverages on a noble metal such as silver, and in particular, on how the adsorption depends upon the orientation of the surface. To obtain the necessary clean flat surfaces, evaporated films of silver have been used here, and single crystals were obtained using epitaxial conditions.

The technique of measurement must be sensitive, because such a study must necessarily involve the use of small areas, since well epitaxed metal films can only be prepared with limited areas, and also the coverages of the adsorbate are likely to be low. A radiochemical technique has therefore been developed to measure the adsorption isotherms under equilibrium conditions by counting, *in situ*, the β-particles from Carbon-14 labeled formic acid molecules adsorbed on the surface. The method was found to be sufficiently sensitive that it could measure about 10^{13} mols./cm^2 on surfaces of a few square centimeters in area. Adsorption measurements were related to the structure of silver films subsequently examined by electron microscopy.

Experimental

The apparatus was designed so that the blank corrections to the count rate for $H^{14}COOH$ molecules in the gas phase, and

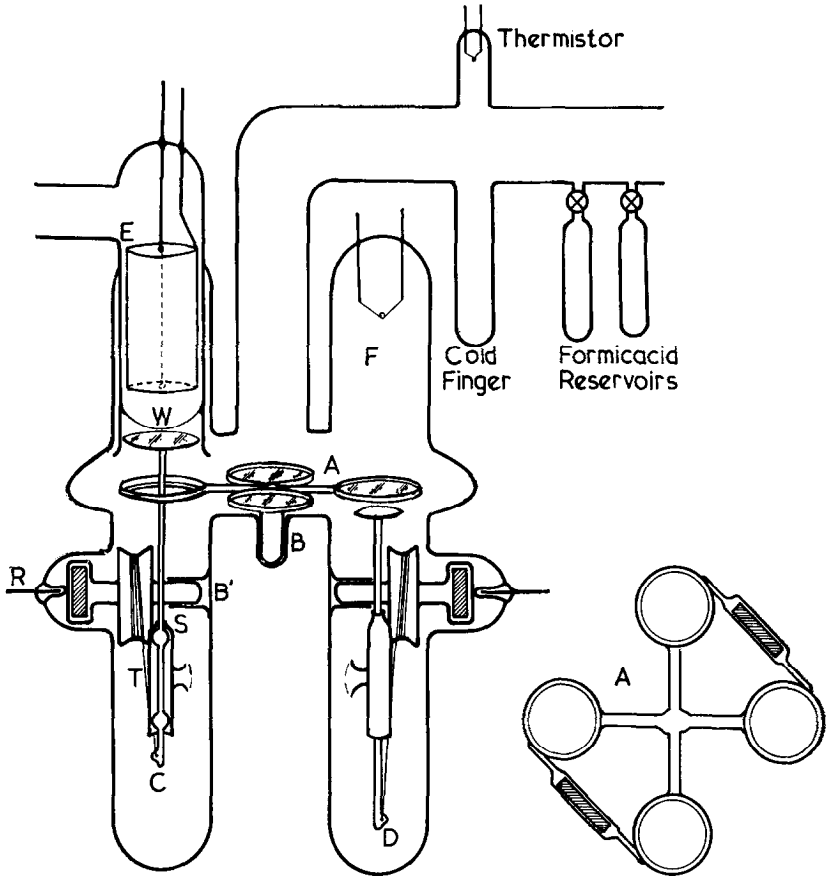

FIG. 1. Details of the adsorption vessel.

adsorbed on the counter window could be evaluated. This was accomplished with the aid of three calibration specimens, and the adsorption vessel was therefore designed so that up to four substrates could be examined in any one adsorption run. In initial experiments, three calibration specimens and a silver substrate were used, and subsequently four silver specimens of different orientation could be examined in the same adsorption run. The apparatus shown schematically in Fig. 1 was made almost completely from Pyrex glass. A tray, A, containing four specimen holders is pivoted about a central bearing, B. Two pistons and magnetically operated winches, C and D, enabled the specimens to be lifted out of the holders and raised up into either tube E containing the counter, or into tube F containing a source for evaporating silver.

Specimens were loaded through the evaporating tube and at the same time the filament was loaded with silver. Winch C contained an iron slug and drum pivoted about the bearing B′. Pt wire, of 0.003-inch/diameter, was wound around the drum with one end attached to the bottom of the piston. A magnet, pivoted about the tungsten rod R, caused the drum to rotate and raised the piston inside the guide T. Eventually a bulge in the piston ground at its upper end fitted into the stop S in the guide T and thereby located the specimen in a fixed position relative to the counter to make the counting geometry reproducible. Winch D did not have this stop.

The counter window, W, was made from thin Pyrex glass about 10 μ thick. The closed end of a tube of 27-mm internal diameter was heated to the melting point and the molten glass sucked into the tube

over a length of about 3 cm until the thin bubble came into contact with a carbon block which molded it into a curved surface. A flat window is desirable because it reduces both the volume of the gas phase between it and the substrate, and its correction. However, flat windows have little physical strength, and a compromise was reached between the strength of the window and the pressure of the gas filling the counter. The most suitable shape was that sketched in Fig. 1. The rounded windows would normally withstand a positive pressure difference of several tens of torr on the concave side, but little difference on the convex side. It was therefore necessary to evacuate the apparatus on both sides of the window simultaneously. The thickness of the window was tested by observing its transparency to ^{14}C β-particles using a commercial counter. The remainder of the counter was constructed from a stainless steel cylindrical cathode with a wall thickness of 0.010 inch and a 0.010 inch diameter tungsten wire as anode. The counter was operated in the proportional region which enabled it to work above room temperature. The most satisfactory pulse distribution was obtained when the counter was filled with 15 torr of methane. The output pulses were fed to a preamplifier, amplifier, discriminator, scaler, rate meter, and pen recorder consecutively.

The counter was calibrated with a standard ^{14}C-labeled disc of poly(methyl methacrylate) with a specific activity of 10 mc/g and a surface β-emission of 2.6×10^4 β/cm^2 min. The area of the disc was the same as that of the specimens. The efficiency of the counter determined from this calibration was usually about 16%. The statistics of counting were arranged so that the standard deviation was never more than 1% of the count.

The remainder of the apparatus consisted of a gas handling system containing metal valves which could be evacuated with an oil diffusion pump and baked at 400°C to produce a background pressure of 10^{-9} torr in the adsorption section, and 10^{-6} torr in the gas handling section. Background pressures were measured with an ion gauge. However, since it is more difficult to prepare epitaxed films of silver on mica under these conditions (*4*), a pressure of between 10^{-6} and 10^{-7} torr was used in the present series of experiments.

Substrates

Adsorption was measured on smooth Pyrex glass, roughened Pyrex glass, mica, polycrystalline silver on Pyrex glass, polycrystalline silver on mica, and (111) epitaxed silver on mica. All specimens were circular with an area of 5.7 cm^2.

Pyrex glass. The specimens were washed with detergent, degreased with methylchloroform, rinsed in acetone, and finally rinsed with distilled water. One pyrex specimen was roughened by abrasion to provide a larger surface area, and then given a similar cleaning treatment.

Mica. Mica specimens were cleaved to either about 3 or 60 mg/cm^2; these will subsequently be called thin and thick mica substrates. The discs were cleaved immediately before being placed in the apparatus, which was then sealed by glass-blowing at F (Fig. 1).

Polycrystalline films of silver on Pyrex. Two methods were used to prepare these films. The Pyrex glass was cleaned, placed in the apparatus, and evacuated without baking (5×10^{-5} torr). The silver was then deposited at room temperature and the whole apparatus was baked at 250°C and evacuated until the pressure dropped to 7×10^{-7} torr. Alternatively, the apparatus was evacuated and baked until the pressure was 7×10^{-7} torr, and then the silver film was deposited on the Pyrex in that vacuum. There was no significant difference in the results obtained on films prepared by these two methods.

Polycrystalline films of silver on mica. These films were deposited on mica at room temperature at a pressure of 5×10^{-5} torr and then the apparatus was baked at 250°C and evacuated until the pressure dropped to 7×10^{-7} torr.

Epitaxed films of silver on mica. Mica was heated to 300°C in a background pressure of 10^{-5} torr, and the silver film deposited in that vacuum, then baked at

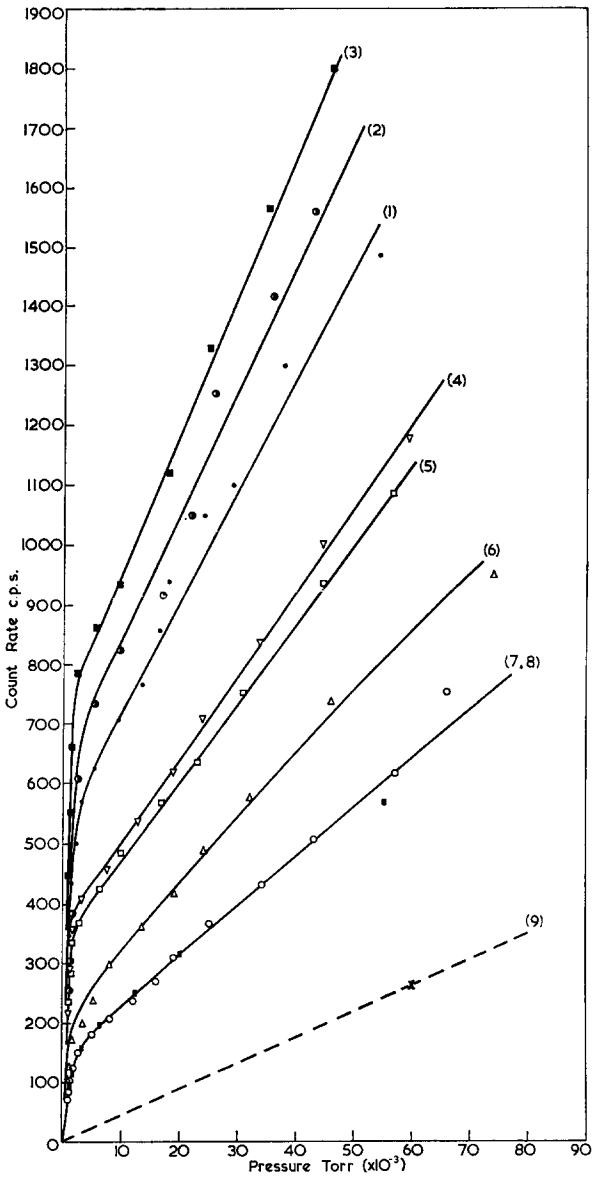

FIG. 2. Variation in count rate with pressure of formic acid admitted to the adsorption vessel: (1) rough glass (RP5); (2) rough glass (RP3); (3) rough glass (RP11); (4) thin mica on smooth glass; (5) smooth glass (P12); (6) polycrystalline Ag on smooth glass (PP10); (7) mica (M9); (8) mica (M14); (9) background gas phase.

250°C, and evacuated until the pressure dropped to 7×10^{-7} torr.

All the silver films were about 1000 Å thick and both the films and their carbon replicas were examined after adsorption with transmission electron microscopy. Scanned electron diffraction patterns were also taken of the (111) epitaxed films. This showed that the structures of the three types of film were similar to those described by Bagg, Jaeger, and Sanders (*5*) as Types 1, 2, and 3.

C-14 Formic Acid

Formic acid (98%) with a specific activity of 21.8 mc/mM from the Radiochemical

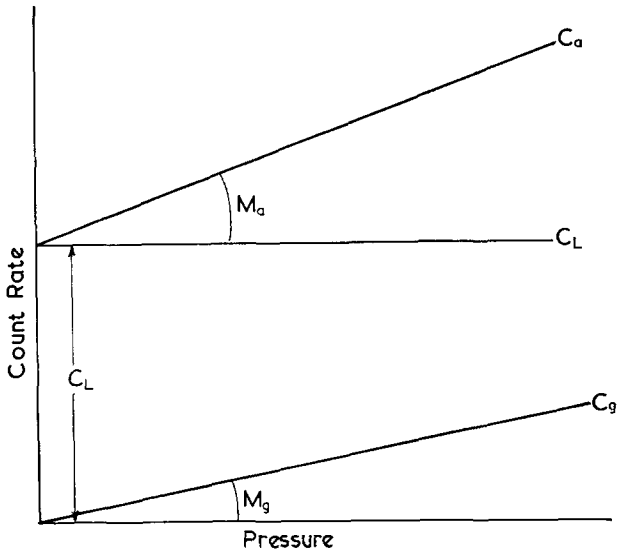

FIG. 3. Schematic representation of the components of the total count rate obtained during isotherm measurement. C_L, C_a, C_g, m_a, m_g are defined in the text.

Centre, Amersham, was stored in a reservoir over a small amount of anhydrous $MgSO_4$.

Any decomposition products which may have formed during storage in the Pyrex container were removed by evacuation at $-100°C$. At this temperature the vapor pressure of formic acid is less than 10^{-5} torr.

Method

Specimens of Pyrex, mica, and silver were prepared as above and located in the tray A of the adsorption vessel (Fig. 1). One specimen was raised out of the tray and located under the counter window. Immediately after purification of the formic acid, an adsorption run was commenced by surrounding the formic acid reservoir with a constant-temperature bath. This gave rise to a constant vapor pressure of formic acid which was allowed to come into contact with the substrate. The rate meter was examined until a constant count rate was achieved, and the value of the count rate was then read from the scaler. Each specimen in the tray was examined in turn and the temperature of the cold bath was then increased in a number of increments as the run proceeded, until a final pressure of about 10^{-1} torr formic acid was reached.

Pressures were measured with a thermistor gauge in the range 10^{-3}–10^{-1} torr, and with a capacitance diaphragm manometer in the range 0.1–20 torr. They were calibrated for formic acid from the known dependence of vapor pressure on temperature, determined in this laboratory, and from the work of Jordan (*6*).

RESULTS

The adsorption isotherms were measured on all substrates at room temperature over a pressure range of 10^{-3} to 10^{-1} torr. At low equilibrium pressures the rate of adsorption was slow, some 10 min or more being required for the system to reach equilibrium. At higher pressures, above 1×10^{-2} torr, equilibrium was attained more rapidly, and above pressures of 3×10^{-2} torr no difference could be detected between the increase in count rate due to pressure increase in the system and that due to attainment of equilibrium.

During an adsorption experiment the total count rate R′ will contain components from three sources: the substrate C_{sub}, the counter window and walls of the adsorption vessel C_w, and the gas phase C_{gas}, i.e.,

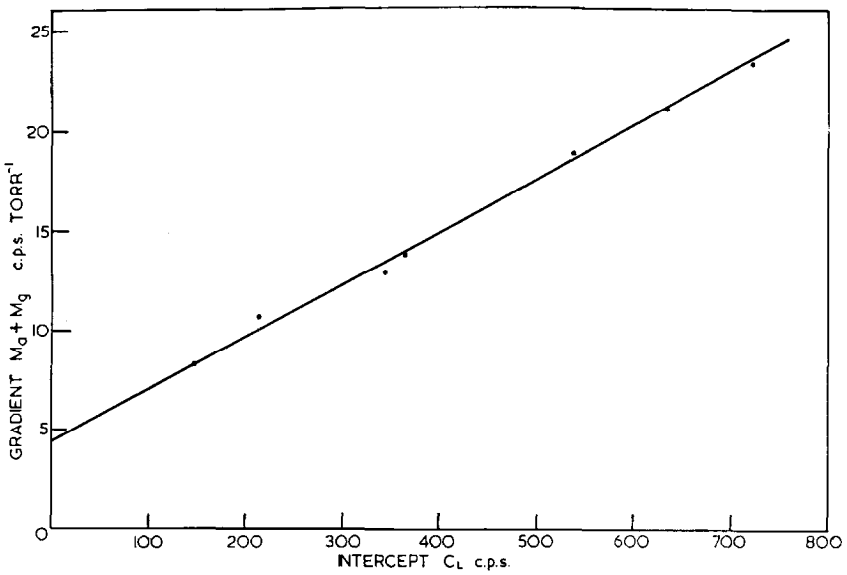

FIG. 4. Variation of the gradients of the linear portions of the isotherms shown in Fig. 2 ($m_a + m_g$) with their intercepts on the count rate axis (C_L).

$$R' = C_{sub} + C_w + C_{gas} \quad (1)$$

Uncorrected R′ isotherms on the various substrates are shown in Fig. 2. Substrates 4, 5, and 7, were the calibration specimens for the window correction. Two independent isotherms are shown for the adsorption on two different samples of thick mica 7, 8 to demonstrate the reproducibility of the measurements.

From the work of Jaffe and Justus (*7*) and Faires and Parkes (*8*), Spink (*9*) has shown that the difference in saturation backscatter of β-particles from substrates of glass and mica, and silver films on these substrates, is negligible. The value of C_{gas} is therefore independent of the substrate, and it will now be shown that C_{gas} can be evaluated from the shape of the isotherms and subtracted from the R' isotherms to give

$$R = C_{sub} + C_w \quad (2)$$

Essentially the total count rate C_T at a pressure P for a substrate i, is represented schematically in Fig. 3, and given by

$$C_T(P,i) = C_L(i) + C_g(P) + C_a(P,i)$$

where C_L is the count rate of the strongly adsorbed layer (pressure-independent since pressure required to form strongly adsorbed layer is very low); C_g, the gas-phase count rate; and C_a, the count rate of weak adsorption beyond that of a Langmuir monolayer. This can be rewritten as

$$\begin{aligned} C_T(P,i) &= C_L(i) + m_g \cdot P + m_a P(i) \\ &= C_L(i) + P[m_g + m_a(i)] \end{aligned}$$

where m_g is the gradient of the gas-phase plot, and m_a, the gradient of the weak adsorption plot. Values of C_L and $(m_g + m_a)$ are obtained from the isotherm plots of C_T versus P. Being a gas-phase contribution, m_g is independent of the substrate present, i.e., $m_g \neq f(C_L)$, whereas m_a may be a function of C_L, i.e., $(m_g + m_a) = m_g + f(C_L)$. A plot of $(m_g + m_a)$ versus C_L for various substrates will therefore yield m_g by extrapolation to $C_L = 0$. This plot is shown in Fig. 4; it is linear, i.e., $m_a = KC_L$ where K is a constant, and gives a good extrapolation to $C_L = 0$. The gas-phase contribution calculated in this way is shown as plot 9 in Fig. 2.

The R' isotherms corrected for the gas-phase contribution give rise to the R isotherms shown in Fig. 5. The error bars arising from the statistics of counting are too small to be shown on the plot.

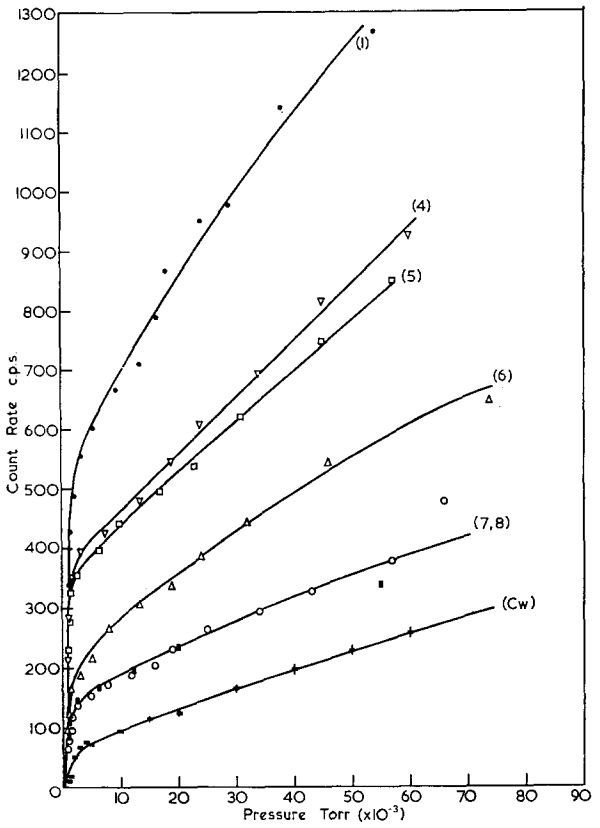

FIG. 5. Adsorption isotherms at 20°C for formic acid adsorption on the counter window (C_w) plus substrates: (1) rough Pyrex (RP5); (4) thin mica on smooth Pyrex; (5) smooth Pyrex (P12); (6) polycrystalline Ag on smooth Pyrex (PP10); (7, 8) thick mica (M9, M14).

In order to correct the R isotherms, the value of C_w was found from the results on the three calibration substrates. The first isotherm was measured on a substrate of smooth Pyrex glass, the total count rate at any pressure consisting of the sum of the contributions due to adsorbate on the window C_w, and on the glass substrate C_g

$$R_g = C_w + C_g \qquad (3)$$

The second substrate was a thin disc of mica placed on top of a Pyrex disc; the total count rate consisted of the components shown in Eq. (4)

$$R_{g2m} = C_w + xC_g + C_m(1 + x) \qquad (4)$$

Here x is a factor allowing for β-particle absorption in the thin mica coming from the adsorbate on the lower side of the mica disc, and from the adsorbate on the glass disc. The value of x was usually about 0.7 and was determined from a plot of the logarithm of transmission versus absorber thickness, using a commercial Geiger counter, Mylar absorbers of varying thickness, and the standard ^{14}C source, in a similar geometrical arrangement to that in the adsorption apparatus.

Finally a thick piece of mica, opaque to 0.158-MeV β-particles, was used as a substrate; this gives a count rate of

$$R_m = C_w + C_m \qquad (5)$$

Equations (3), (4), and (5) can now be solved for C_w

$$C_w = 0.5[R_g + R_m - (R_{g2m} - R_m)/x] \qquad (6)$$

The three calibration isotherms (Fig. 5, curves 4, 5, and 7) were applied to Eq. (6) to give an isotherm due to adsorption on

the counter window. This isotherm is also shown in Fig. 5, labeled C_w. As a result of the correction incurred by Eq. (6), the statistical error bars for C_w are now larger and are shown in Fig. 5. This C_w isotherm was now subtracted from the R isotherms, giving the true substrate isotherms (Fig. 6). A similar treatment for the adsorption

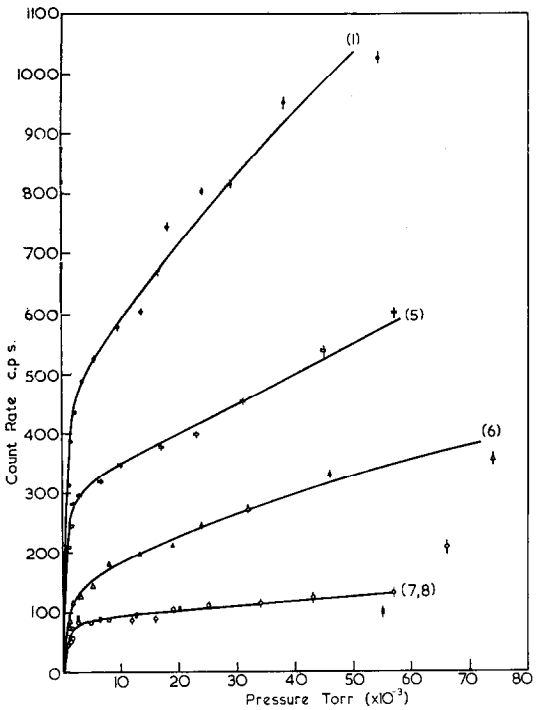

FIG. 6. Adsorption isotherms at 20°C for formic acid adsorption on (1) rough Pyrex (RP5); (5) smooth Pyrex (P12); (6) polycrystalline Ag on smooth Pyrex (PP10); (7, 8) thick mica (M9, M14).

on smooth Pyrex glass (P12), polycrystalline films of silver on Pyrex glass (PP46), polycrystalline films of silver on mica (PM46, PM37), and (111) epitaxed films of silver on mica (SM46, SM36) gives the true substrate isotherms shown in Fig. 7. The result on Pyrex from Fig. 6 is included for comparison, but the results on silver were from different runs than those in Fig. 6. Results PP46, PM46, SM46, were obtained during the same adsorption run by making use of the facility of the apparatus for containing up to four substrates.

It is unfortunate that the adsorption on the Pyrex counter window causes such a large correction. However, the counting statistics have been arranged so that the error in this correction is less than 5%. Errors arising from differences in adsorption on the counter window from one run to another can be minimized by using the same window throughout a series of runs, and by comparing different substrates during the same adsorption run (for example, runs PP46, PM46, SM46). Comparison of these results with results PM37 and SM36, obtained from separate adsorption runs, shows that the reproducibility is still reasonable from one run to another (about 8%).

In the subsequent results and discussion we shall be concerned only with corrected isotherms and therefore true adsorption. Langmuir plots have been made for all the isotherms, and Fig. 8 shows some of these for substrates of Pyrex, polycrystalline silver on mica, and (111) epitaxed silver on mica. For comparison, Freundlich plots are also shown inset. The Langmuir plots are linear over the lower part of the total pressure range, but above 2×10^{-2} torr the slope changes. The initial slope at low pressures can be used to measure saturation values of the surface coverage. From the specific activity of the ^{14}C formic acid and the geometrical area of the substrates,

TABLE 1
MONOLAYERS OF FORMIC ACID ADSORBED ON VARIOUS SUBSTRATES

Substrate	Number of mols./cm² × 10¹³	Area/ mols. (Å)	Ratio of covered atoms to total atoms per area
Pyrex	27	37	—
Rough Pyrex	52	20	—
Pyrex	22.3	45	—
Pyrex	25.2	40	—
Mica	7.2	139	—
Poly Ag Pyrex (PP10)	16.3	61	1:9
Poly Ag Pyrex (PP44)	16.4	61	1:9
Poly Ag Pyrex (PP46)	17.7	57	1:9
Poly Ag mica (PM37)	14.8	68	1:11
Poly Ag mica (PM46)	15.2	66	1:11
Single Ag mica (SM46)	8.7	115	1:17
Single Ag mica (SM36)	9.4	106	1:17

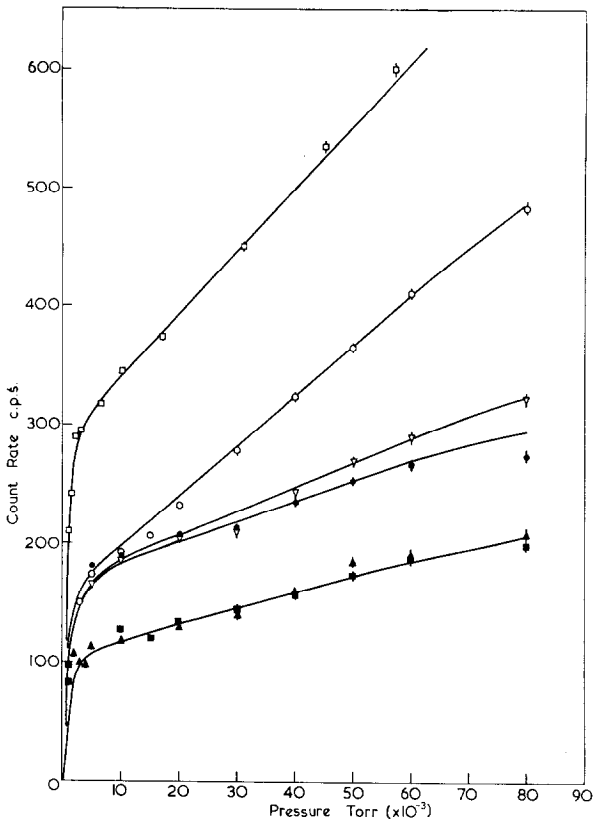

FIG. 7. Adsorption isotherms at 20°C for formic acid adsorption on Pyrex glass (□, P12); polycrystallina Ag on Pyrex (○, PP46); polycrystalline Ag on mica (●, PM37; ▽, PM46); (111) epitaxed Ag on mice (■, SM36; ▲, SM46).

the count rates can be converted into numbers of molecules/cm². These values are shown in column 2 of Table 1, and column 3 of Table 1 shows the coverages expressed as areas of the surfaces per formic acid molecule adsorbed. Again, assuming that the real area equals the geometric area, column 4 shows the proportion of atoms in the surface covered with formic acid to the total number in a given area. As a reference to the size of the formic acid molecule, Table 2 shows the areas of the formic acid molecule calculated in different ways: (i) assuming that the molecule is adsorbed as an ion with the bond resonating between the two oxygen atoms; rotation is possible about the C–H axis normal to the surface, and the area is that swept out by the molecule as it rotates; (ii) assuming that the molecule is immobile and the area is that of the rectangle which just encloses the projected area of the molecule when it is bonded to the surface through the OH group; (iii) calculated from the average volume of the molecule in the solid state and assuming the same projection on to the surface as in (ii).

TABLE 2
CALCULATED AREAS OF FORMIC ACID MOLECULES

Areas of formic acid		
Ion rotating about surface bond	Immobile ion	Calculated from average volume in solid state
9.6 Å²	5.5 Å²	12.5 Å²

During one adsorption run, when the pressure of formic acid reached 5×10^{-3} torr, the gas phase was removed by evacuation at room temperature and the count rate from the surface was examined. No

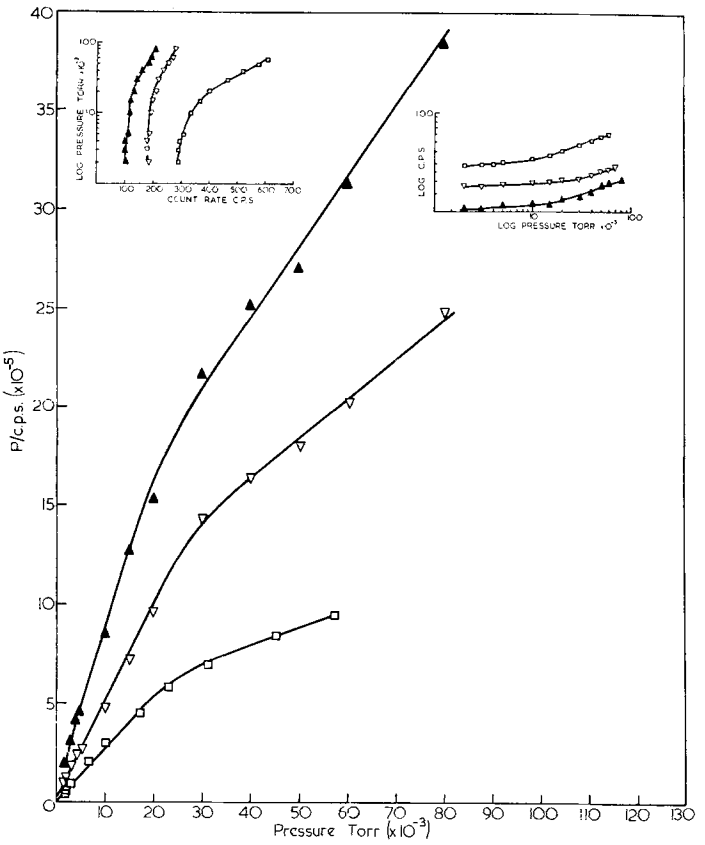

FIG. 8. Langmuir plots; adsorption of formic acid on Pyrex glass (□, P12); polycrystalline Ag on mica (▽, PM46); (111) epitaxed Ag on mica (▲, SM46). Inset are Freundlich and Temkin plots for the same substrates.

change in count rate was observed other than that due to removal of the gas phase. At the completion of every adsorption run, the gas phase was always condensed back into the formic acid reservoir at −196°C, and the count rate examined. The change in count rate was greater than that due to removal of the gas phase alone. The count rate arising from adsorption on the counter window, given by the calibration procedure, was subtracted from these values. This gave the substrate count rate, which showed that a weakly adsorbed portion of the adsorbed layer had been removed, leaving a strongly adsorbed portion which could not be removed by prolonged evacuation at room temperature. The magnitude of the strongly adsorbed portion corresponded to the coverage values shown in Table 1.

DISCUSSION

During an adsorption run, if the gas phase is removed at pressures less than 5×10^{-3} torr no change in adsorption on the surface occurs. At low pressures, therefore, the adsorption is strong and irreversible at room temperature. At the end of an adsorption run, when the gas phase is removed at pressures of 1×10^{-1} torr, a weakly adsorbed portion of the layer is removed, leaving a strongly adsorbed portion of the same extent as the coverage shown in Table 1. It appears, therefore, that there are two types of adsorption present on the surface.

The Langmuir plots are linear at low pressures, but fall off from linearity above pressures of 2×10^{-2} torr. Freundlich, or Temkin isotherms give a similar result. The coverages evaluated from this linear portion of the plot therefore describe the coverages of the strongly adsorbed species. It is possible that the change in slope of the plot is due to the buildup of the weakly adsorbed species on the surface at higher pressures.

Table 1 shows that the coverage on glass is larger than that on the silver films. Results on the silver specimens show that the value of the coverage decreases as the proportion of the surface which is (111) increases. There is little difference in the coverage on surfaces of polycrystalline silver deposited on Pyrex, and on mica. This agrees with the results of Jaeger (*10*), who found little difference in the preexponential factor or activation energy for formic acid catalysis on these two types of film.

The (111) grains in the films can be distinguished in electron micrographs, and hence the proportion of the surface which is (111) can be estimated from a number of random electron micrographs. Values for the films used here are 90% (111) for epitaxed silver, 30% (111) for polycrystalline silver on mica, and 10% (111) for polycrystalline silver on Pyrex. Using these values, together with their respective coverage values of 9×10^{13}, 15×10^{13}, and 17×10^{13} mols./cm^2, a set of equations can be set up with $a_{(111)}$ = (111) area, and a_r = rough area:

$$0.9a_{(111)} + 0.1a_r = 9 \times 10^{13} \text{ mols./cm}^2$$

$$0.3a_{(111)} + 0.7a_r = 15 \times 10^{13} \text{ mols./cm}^2$$

$$0.1a_{(111)} + 0.9a_r = 17 \times 10^{13} \text{ mols./cm}^2$$

These give coverage values for the (111) plane alone, and the rough surface alone. The three equations are consistent with each other, and give values of 18×10^{13} mols./cm^2 for the rough surface, and 8×10^{13} mols./cm^2 for the (111) plane; i.e., the ratio of HCOOH to Ag atoms is 1:5.5 on the rough surface, and 1:12.5 on the (111) plane. The value for the rough surface of silver is similar to that obtained by Sachtler and Fahrenfort (*3*) for the adsorption on polycrystalline gold under similar conditions, i.e., 1:4.

It is realized that the values calculated above depend on the accuracy of the estimates of (111) areas present in the specimens, but clearly, regardless of any errors, the coverage on the (111) plane is very low. On such a close-packed plane, rotation of the adsorbed ion about the bond from the surface to an oxygen atom is likely; this would effectively block off six other metal atom sites from adsorption of other ions. Baker (*11*) has shown that for adsorption of large atoms on hexagonal crystals [e.g., the atoms of a (111) plane] when the coverage becomes high enough, multiple blocking of sites occurs. The maximum coverage which can be attained with these large atoms has been calculated by Baker for the case of sequential filling of the surface. Here, the maximum coverage was calculated to be one adsorbate atom to every 4.5 metal sites. Sequential filling of the surface is likely for the case of the strongly adsorbed formate ions, and hence a coverage of 1:4.5 is the maximum to be expected for the adsorption of these ions with preserved rotation. On the (111) plane the coverage is considerably lower than would be expected from a freely rotating ion, and there is little multiple blocking of sites. The explanation of the low coverage must, therefore, lie in the influence of the adsorbed ion on other potential sites. Perhaps consideration of the degree of overlap of the bonding molecular orbitals in the formate ion with those of the metal atoms in the (111) plane might lead to a better understanding of the situation. This type of treatment has been considered by Bond (*12*) for adsorption of unsaturated hydrocarbons on metals. In the case of the rough surface, the coverage of 1:5.5 is that to be expected from the adsorption of a freely rotating ion. The lack of highly energetic sites on the (111) plane could account for the change in adsorption from the maximum value expected for a

freely rotating ion on the rough surface to the much lower value on the (111) plane. A change in surface area alone would not account for this difference.

Acknowledgments

The author would like to thank Dr. J. V. Sanders for his help in the interpretation of electron micrographs and for much useful discussion. Mr. Jost Kaiser deserves considerable credit for his glass-blowing skill in the manufacture of the adsorption vessel.

References

1. Fahrenfort, J., Van Reigen, L. L., and Sachtler, W. M. H., "The Mechanism of Heterogeneous Catalysis" (J. H. de Boer, ed.), p. 23. Elsevier, Amsterdam, 1960.
2. Tamaru, K., *Trans. Faraday Soc.* **55**, 824, 1191 (1959).
3. Sachtler, W. M. H., and Fahrenfort, J., *Actes Congr. Intern. Catalyse, 2e, Paris, 1960*, p. 83 (Edition Technip, Paris, 1961).
4. Jaeger, H., Mercer, P., and Sherwood, R., *Surface Sci.* **6**, 309 (1967).
5. Bagg, J., Jaeger, H., and Sanders, J. V., *J. Catalysis* **2**, 449 (1963).
6. Jordan, T. E., "Vapour pressure of Organic Compounds," p. 121. Interscience, London, 1954.
7. Jaffe, L., and Justus, K. M., *J. Chem. Soc.*, p. S341 (1949).
8. Faires, R. A., and Parkes, B. H., "Radioisotope Laboratory Techniques," p. 223. Newnes, London, 1958.
9. Spink, J. A., *J. Colloid Interface Sci.* **23**, 9 (1967).
10. Jaeger, H., *J. Catalysis* **9**, 237 (1967).
11. Baker, B. G., *J. Chem. Phys.* **45**, 2694 (1965).
12. Bond, G. C., *Discussions Faraday Soc.* **41**, 200 (1966).